Undercooling-induced metastable $A15$ phase in the Re-W system from drop-tube processing

S. Tournier and B. Vinet
Commissariat à l'Énergie Atomique, CEREM-Département d'Étude des Matériaux, 17 rue des Martyrs, 38054 Grenoble, France

A. Pasturel
CNRS, Laboratoire de Physique Numérique des Systèmes Complexes, 25 rue des Martyrs, 38042 Grenoble, France

I. Ansara and P. J. Desré
INPG-CNRS-UJF, Laboratoire de Thermodynamique et Physico-Chimie des Matériaux, Boîte Postale 75, 38402 Saint-Martin-d'Hères, France

(Received 18 April 1997; revised manuscript received 17 October 1997)

An $A15$ metastable phase is involved in the solidification path of undercooled Re-W alloys in a tremendously wide range of compositions (from 34 to 82 at. % W). The melting temperature of the $A15$ phase reaches 3250 K at 75 at. % W. First-principles calculations were performed to determine the structural stability of the $A15$ phase in this system. A value of 3200 K is deduced for the melting temperature of the $A15$-(W) which thus appears to be the true β phase of this element. The metastable liquid-$A15$ phase diagram, that fits well the experimental results, is computed by the Calphad method assuming a two sublattice description of the $A15$ structure to simulate order-disorder phenomena.
[S0163-1829(98)00806-6]

I. INTRODUCTION

Nucleation experiments are mainly realized on low melting point materials by dividing the melt into tiny discrete droplets. The undercooling amount of 900 K achieved on bulk Re droplets in the Grenoble drop-tube appears to be a promising result.[1] Statistical analysis of the nucleation events gives confidence in a homogeneous nucleation process for W, Re, Ta, Mo, Nb, and Ir. Each amount of undercooling is interpreted in the framework of the classical theory of nucleation and consequently the limit of the metastable liquid state is shown to be an intrinsic property of the material.[2] From a chemical point of view, heterogeneous nucleation can be bypassed in these experiments thanks to the strong initial purification of the droplet under ultrahigh-vacuum conditions (10^{-7} Pa) as well as the lack of stable oxides for these metals at the measured nucleation temperatures.

The interest in drop-tube processing is also highlighted as giving, to our knowledge, the first experimental evidence of an undercooled-induced metastable phase transformation in pure transition metals.[3] The coupling of these experiments with *ab initio* calculations allows us to identify the transitory phases, namely the fcc and $A15$ phases for Re and Ta, respectively. Agreement is found through a comparison of their measured and calculated melting temperatures.

The experimental program on alloys has been focused on systems showing complex σ ($D8_b$) and χ ($A12$) phases which may be obtained by associating a hcp metal such as Re with bcc metal such as W, Mo, Ta or Nb. In this paper, emphasis is put on the pronounced nonstoichiometric behavior found for the metastable $A15$ phase in the Re-W system at very high temperatures. This study is of a particular interest since the $A15$ structure is often regarded as belonging to a group of structures characterized by well-defined stoichiometric ratios.

II. EXPERIMENTAL METHOD

At the top of the 48 m high facility, droplets of a few millimeters in diameter are prepared from a wire by using the pendant drop technique with electron-bombardment heating.[4] Alloy droplets are made by shifting the composition of a commercial wire (W, 5 at. % Re, 26 at. % Re or Re) by adding locally an appropriate mass of a wire chosen among the same products. They are received either onto a damping plate or into shot tin to improve cooling efficiency for a better preservation of the as-solidified microstructure. After nucleation there is recalescence and the monitoring of this event, due to the release of the heat of crystallization, leads to the possibility of determining the nucleation and the post-recalescence temperatures. The brightness of the droplet is tracked by a series of high-speed silicon diodes installed along the tube. Measuring the time t_n between the droplet release and the nucleation event, the nucleation temperature T_n is calculated via a numerical integration of the cooling rate V

$$V=\frac{dT}{dt}=-\frac{\varepsilon_t(T)\sigma}{C_p(T)}\,T^4\left[\frac{36\pi}{m\rho^2(T)}\right]^{1/3}, \tag{1}$$

which takes into account linear evolutions of liquid density ρ, heat capacity C_p, and hemispherical emissivity ε_t with temperature. σ is the Stephan-Boltzmann constant. Average values are considered for emissivity and heat capacity based on atomic percentage (see Ref. 5 for the used data). Even if the typical accuracy on T_n is ± 30 K, the *time* approach allows a resolution in temperature of a few K due to an uncustomary reproducibility under ultrahigh-vacuum conditions of both the mass and the initial temperature of the falling droplets. Within the experimental environment, the initial temperature identifies with the liquidus temperature T_L of the alloy with a constant overheating of about 10 K. An excel-

lent definition of the curve of the maximum undercooling versus composition (T_n curve) is then obtained explaining the possibility for attempting meaningful statistical analysis of nucleation events.

The post-recalescence temperature $T_{\rm pr}$ is inferred through a single color pyrometry approach from the height of the recalescence peak by application of Wien's law leading to

$$T_{\rm pr}^{-1}=T_n^{-1}-\frac{\lambda}{C_2}\left[\ln\frac{S(T_{\rm pr})}{S(T_n)}\right]. \qquad (2)$$

λ is the used wavelength (853 nm) and C_2 is the second radiation constant. $S(T)$ is the signal delivered by the diode. Simplifications are made considering that the droplet is quite motionless during the very short recalescence duration ($\approx$1 ms). Moreover, the spectral emissivity $\varepsilon(\lambda,T)$ is assumed to be constant during recalescence since λ is chosen in the vicinity of the so-called X points of Re at which spectral emissivity does not change with temperature.[6]

When $T_{\rm pr}$ is known, the *pyrometric* approach may allow the determination of the nucleation temperature. However, in the course of the present study, this method is not suitable because of the occurrence of numerous metastable phenomena as well as the hypercooling regime imposed by Re (undercooling $\Delta T=T_L-T_n$ is higher than the ratio of the heat of the crystallization by the liquid heat capacity). It could be only applied in a small composition range, between 82 at. % W and pure W, where the post-recalescence temperature is found to reach the solidus temperature T_s (isenthalpic regime). This last result confirms the terminal curves relative to the (W) solid solution drawn by Massalski *et al.*[7] on the basis of the experimental work of Dickinson and Richardson.[8]

Let us finally indicate that two kinds of droplets may result from large liquid undercoolings. The first kind, which forms the majority, corresponds to the samples exhibiting the same amount of deep undercooling (for a given composition) in agreement with a homogeneous nucleation process. The second kind of droplet results from heterogeneous nucleation events due to the remaining impurities of very small size within the falling liquid. Obtaining so-called *singular* droplets is of particular interest since the formation of a metastable phase may be thermodynamically favored [e.g., the discovery of metastable phases for Re and Ta (Ref. 3)]. Unfortunately, their preparation is not yet controlled (inoculation could be a possible way to reproduce the nucleation path).

III. EXPERIMENTAL RESULTS

Figure 1 summarizes the undercooling results obtained on the Re-W system. With the increase of W content, the nucleation temperature T_n is quite constant, while the post recalescence temperature $T_{\rm pr}$ decreases significantly. A straightforward calculation of the limit for the hypercooling regime is realized in the frame of a simple regular solution approximation by taking an interaction parameter λ equal to $-16\ {\rm kJ\,mol^{-1}}$ according to De Boer *et al.*[9] The deduced composition of 32 at. % W corresponds to the first inflexion point i_1 of the T_n curve. The temperature gap δT goes through a minimum ($\approx$330 K) at 15 at. % W, i.e., near the

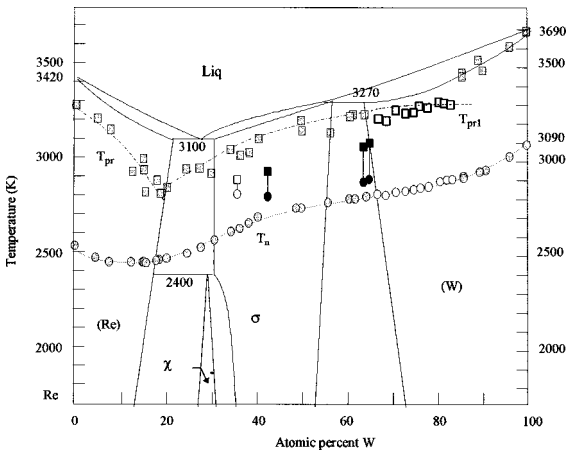

FIG. 1. Undercooling results obtained on the Re-W system: the circles correspond to the nucleation temperatures and the squares to the post-recalescence temperatures; single recalescence events relative to the maximum (grey) or lower (black) amount of undercooling, first peak of double recalescence phenomena (white).

theoretical value of 16.7 at. % W determined for the maximum difference between the enthalpies of the fusion of Re and of the alloy assuming partitionless solidification. As analyzed elsewhere,[10] a metastable (W)-bcc phase nucleates primarily within the σ-phase domain; the stable σ-phase results from a solid-state transformation. The inflexion point i_2 near 60 at. % W corresponds to the end of this metastable behavior. From 65 to 82 at. % W, brightness traces show systematically a double recalescence phenomenon (Fig. 2). The nucleation temperatures T_{n1} of the first recalescence event take place on the T_n curve, while the respective $T_{\rm pr1}$ temperatures are quite constant around 3250 K. The temperature gap for the second peak δT_2 increases with W content, from detectable at 65 at. % W up to $\approx$120 K at 75 at. % W, while the time between the two events decreases significantly from $\approx$330 ms down to $\approx$180 ms (Fig. 3). Finally, from 82 at. % W to pure W a sole recalescence event is detected corresponding to the nucleation of the stable (W) solid solution.

X-ray-diffraction analysis of the droplets showing the double recalescence phenomenon observed between 65 and 82 at. % W leads to patterns corresponding to the stable (W) solid solution. It does not give information on the nature of the transitory metastable phase. Nevertheless, some *singular* droplets are obtained in the course of this work with the realization of a double recalescence event characterized by a

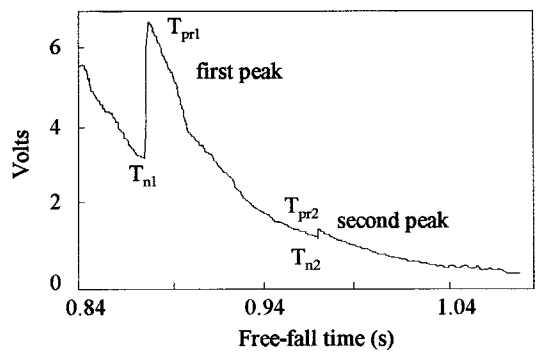

FIG. 2. Detector output signal showing a double recalescence phenomenon at 74 at. % W.

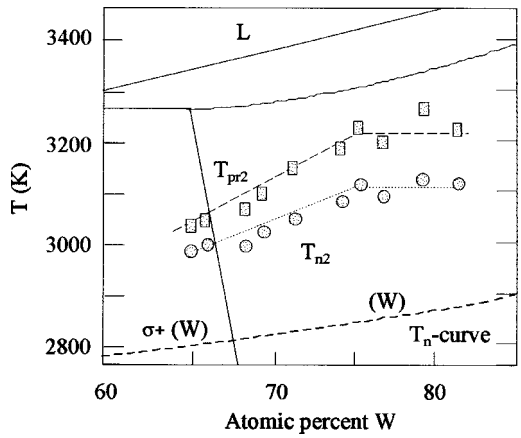

FIG. 3. Nucleation (circles) and post-recalescence (squares) temperatures corresponding to the second peak of the double recalescence events obtained between 65 and 82 at. % W.

short time ($\approx$10 ms) between the two peaks at 34 at. % W, and sole recalescence events at 40 and 63 at. % W (see Figs. 1 and 6). The same x-ray-diffraction analysis then reveals the presence of the $A15$ phase together with the stable σ phase at 40 at. % W (Fig. 4) and the (W) solid solution at 63 at. % W. As the stoichiometric composition of the $A15$ phase corresponds to 75 at. % W, it is thus tempting to suppose that this phase is involved in the observed metastable phenomenon. Besides, only a part of the droplet is solidified at the end of the first recalescence event. The possibility for the liquid to remain undercooled depends on wetting conditions between the liquid and solid which are obviously controlled by the nominal composition when considering the significant time evolution between the two recalescence peaks (see Fig. 3). The lack of a second peak at compositions below 65 at. % W is consistent with a complete droplet solidification into the metastable phase which makes it easier to be found by x-ray-diffraction analysis.

IV. ANALYSIS

A metastable $A15$ phase in the Re-W system has already been reported by Federer and Steele[11] between 55 and 87 at. % W using a vapor deposition technique near 800 K. A mixing of $A15$ and σ phases has also been found by Khusainov *et al.*[12] on a deposited 50 at. % W alloy. Furthermore, the discovery of the $A15$-Ta phase after a modest undercooling led us to expect a similar situation for W. The main finding of the drop-tube experiments on the Re-W system is thus to reveal the extraordinary extension in composition, at very high temperature, of the $A15$ phase metastability.

A thorough knowledge into the physics of the observed metastable behavior is gained through calculations from the first-principles full potential linear muffin-tin orbitals method (FPLMTO). This approach,[13] one of the most accurate within the local-density approximation (LDA), is an all-electron method, which does not require any shape approximation for density and potential. Particular care is taken in this work for the total-energy convergence, due to the k-space integration, which is done by application of a special k-point technique.[14] The smearing parameter is chosen to be 0.1. For the full potential, LMTO's are used with various localizations: 34 augmented Hankel functions per Re and W site $[s(3k\text{'s}),\ p(3k\text{'s}),\ d(3k\text{'s}),\ f(1k\text{'s})]$ are considered where the corresponding decay energies (in Ry) are $-k^2=-0.01\,(spdf),\ -1.0(spd),\ -2.3(spd)$. Accurate predictions are gained by including a second ''semicore'' panel which provides bandlike treatments of both the $5s$ and $5p$ states for Re and W.[15] All the reported LDA results are scale-relativistic calculations using the exchange-correlation potential of Ceperley and Adler.[16]

The energies of formation of the ground-state structures, namely χ and σ phases, are calculated as well as the energies of formation of the $A15$ structure for Re, W, ReW_3, and Re_3W compounds (Fig. 5). It is shown that the ReW_3 compound takes place just above the line drawn between the energies of σ and pure bcc-W (reference) structures, revealing the metastable character of the $A15$ structure at this composition. The Re_3W compound is particularly unstable displaying a positive energy of formation. Linking the different values of the $A15$ energy of formation, zero is found at 66 and 89 at. % W. In this composition range, the solidification path is really shown to involve systematically the primarily formation of the metastable $A15$ phase, while heterogeneous nucleation is needed to induce this phase for other compositions. Using the value of the lattice stability of W and Re in the A15 structure and supposing that the entropy of melting of the A15 phase and (respectively) of the stable bcc and hcp phases are similar, a straightforward thermodynamic calculation leads to $T_{m\text{-met}}^{(A15\text{-W})}=3225$ K and $T_{m\text{-met}}^{(A15\text{-Re})}=1570$ K. The extrapolation of the T_{pr1} curve gives a melting temperature for the $A15$-W phase of $\approx$3220 K in good agreement with

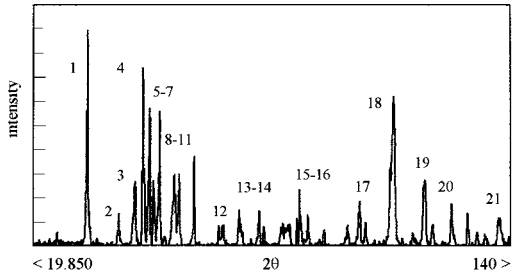

	1	2	3	4	5	6	7	8	9	10	11	12	13	14	15	16	17	18	19	20	21
A15	111	200		210			211			222				222	321	400	420	421	520	521	440
σ			410		212	411		222	312		431	432	621								

FIG. 4. X-ray-diffraction pattern obtained for a 40 at. % W droplet (table gives the peak indexation) using K_α cobalt radiation ($\lambda_{Co}=0.17903$ nm).

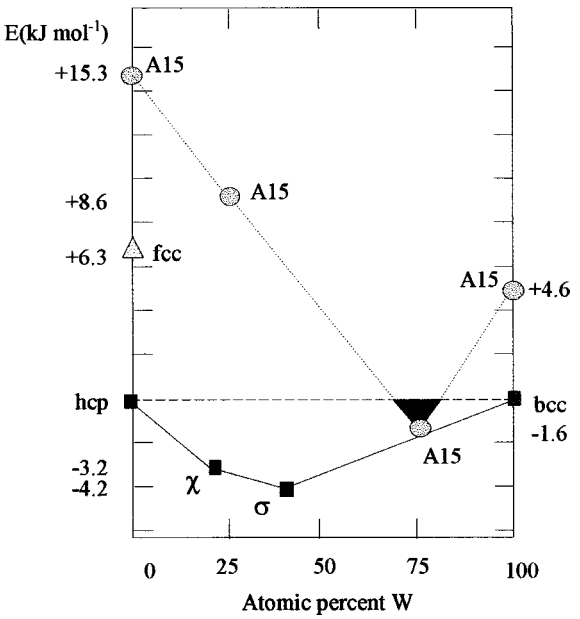

FIG. 5. Calculations by FPLMTO's method of the structural energy of σ, χ, and $A15$ phases in the Re-W system.

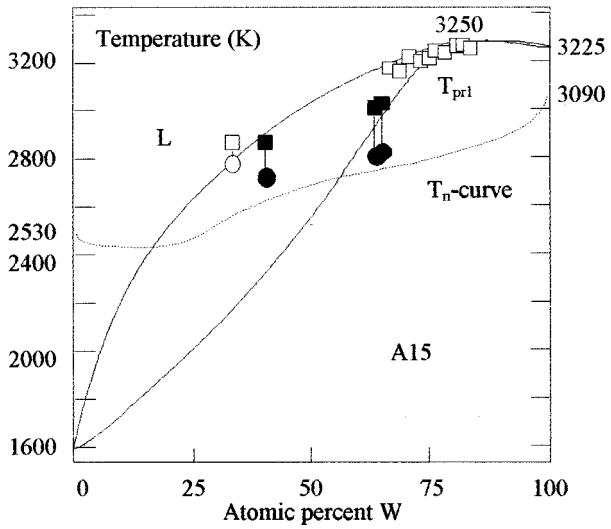

FIG. 6. Phase diagram between the liquid and the $A15$ phase established through the hypothesis that the $A15$ phase behaves as a solid solution with two sublattices in the Re-W system.

the estimated value. As for pure Ta, the $A15$ alternative phase can be reached after a modest normalized undercooling of $\approx 0.13 T_m^{\mathrm{bcc}}$.

A better understanding of the undercooling results may be obtained by calculating the metastable phase diagram involving the liquid and the $A15$ phases. In the absence of any experimental information of their thermodynamic properties, several assumptions are made to evaluate them. For the pure elements, combining the enthalpy of transformation Re-hcp→Re-$A15$ and W-bcc→W-$A15$ as derived from first-principles calculations to the Gibbs energy of fusion of the pure elements Re and W (respectively, equal to 15.3 and 4.6 kJ mol^{-1}), the Gibbs energy of the metastable liquid-$A15$ transformation is deduced for both elements. For the liquid phase, a regular solution model is used. The interaction parameter is derived from the evaluation of De Boer *et al.*[9] (-4000 J mol^{-1} at 50 at. % W). The $A15$ stoichiometric compound is assumed to be formed of two sublattices—in agreement with crystallography—with an ideal mixture of the elements on each of them. The phase can then be modeled as $(\mathrm{Re}_{u1}\mathrm{W}_{u2})(\mathrm{Re}_{v1}\mathrm{W}_{v2})_3$ where u_i and v_j are the site fraction of the elements i and j ($u_1+u_2=v_1+v_2=1$). For the model, the Gibbs energy of formation is described by the equation below:

$$G_m = u_1 v_1 G_{\mathrm{Re:Re}} + u_2 v_2 G_{\mathrm{W:W}} + u_1 v_2 G_{\mathrm{Re:W}} + u_2 v_1 G_{\mathrm{W:Re}} + G^{id},$$

with

$$G^{id} = RT\left(\sum_{i=1}^{2} u_i \ln u_i + 3 \sum_{j=1}^{2} v_j \ln v_j \right), \qquad (3)$$

where $G_{i:j}$ are the Gibbs energies of the ideal compounds and $G_{i:i}$ that of the pure elements. The enthalpies of formation of the metastable ReW_3 and $\mathrm{Re}_3\mathrm{W}$ are these derived here from first-principles calculations. The entropies of formation are assumed to be zero, which corresponds nearly to a weighted sum by the stoichiometric number of the entropies of the pure elements. An entropy regular solution parameter for the liquid phase taken equal to 2.2 J mol^{-1} T^{-1} is used to account for a congruent melting equilibrium in the W-rich side as could be suggested from the experimental observations. The metastable phase diagram is calculated with the THERMO-CALC software package.[17] A reasonable interpretation of the experimental results (Fig. 6) is obtained with the two sublattice descriptions: each post-recalescence temperature of the original and double recalescence droplets takes place near the liquidus line of the calculated diagram; the T_{pr1} temperatures are inside the metastable zone liquid-$A15$.

The high degree of atomic order of the tetrahedral close-packed structures (or Frank-Kasper phases) usually results from a dominant size factor in driving their stability. Nevertheless, in a few cases, the geometrical factors are not dominant, thus allowing the formation of substitutional solid solutions or ''electron phases'' in a broad composition range.[18] As suggested by van Reuth and Waterstrat[19] and more recently examined by Turchi and Finel[20] this situation can be met for the $A15$ structure. However, from an experimental point of view, nonstoichiometric $A15$ phases only appear in the equilibrium phase diagram of a few refractory systems [e.g., Os-V (Ref. 7)]. The present investigation on the Re-W system shows a tendency for $A15$ phase formation over the broadest compositional range yet reported. This behavior can be viewed as the competition between thermal effects and energetic contributions.[21] The Re-W system develops weak heteroatomic interactions since the formation energies of the different stable phases namely σ and χ phases display small negative values. The weaker the heteroatomic interactions, the more important the predominance of entropic effects, the formation of solid solutions. This is also the case for the metastable $A15$ structure which is favored by the nucleation path in a tremendously wide range of composition.

ACKNOWLEDGMENTS

The experimental work has been conducted within the framework of the G.R.A.M.M.E. agreement between the

C.E.A. and C.N.E.S. This investigation is also part of a research program sponsored by the E.S.A. under Contract No. 9638/91/NL/JSC. The first-principles calculations are supported by a computer grant at the Institut du Développement et des Ressources en Informatique (I.D.R.I.S.-C.N.R.S.). The authors would like to thank J.C. Idelon and P. Sibellas for their technical assistance. It is a pleasure to acknowledge the help of C. Martin.

[1] B. Vinet, L. Cortella, P. J. Desré, and J. J. Favier, Appl. Phys. Lett. **58**, 97 (1991).
[2] L. Cortella and B. Vinet, Philos. Mag. B **71**, 11 (1995).
[3] L. Cortella, B. Vinet, P. J. Desré, A. Pasturel, A. T. Paxton, and M. van Schilfgaarde, Phys. Rev. Lett. **70**, 1469 (1993).
[4] B. Vinet, J. P. Garandet, and L. Cortella, J. Appl. Phys. **73**, 3830 (1993).
[5] B. Vinet, L. Cortella, and A. Boch, Trans. Mat. Res. Soc. Jpn. **16A**, 593 (1994).
[6] J. P. Hiernaut, R. Beukers, M. Hoch, T. Matsui, and R. W. Ohse, High Temp.-High Press. **18**, 627 (1986).
[7] *Binary Alloy Phase diagrams*, edited by T. B. Massalski, H. Okamoto, P. R. Subramanian, and L. Kacprzak (American Society for Metals, Materials Park, OH, 1990).
[8] J. M. Dickinson and L. S. Richardson, Trans. Am. Soc. Met. **51**, 758 (1959).
[9] F. R. De Boer, R. Boom, W. C. M. Matteus, A. R. Miedema, and A. K. Niessen, in *Cohesion in Metals, Transition Metal Alloys*, edited by F. R. de Boer and D. Pettifor (North-Holland, Amsterdam, 1988).
[10] S. Tournier, M. Barth, D. M. Herlach, and B. Vinet, Acta Mater. **45**, 191 (1997).
[11] J. I. Federer and R. M. Steele, Nature (London) **205**, 587 (1965).
[12] M. A. Khusainov, Yu. V. Lakhotkin, D. M. Umidov, and A. I. Krasovskiy, Russ. Metall **4**, 176 (1981).
[13] M. Methfessel, Phys. Rev. B **38**, 1537 (1988).
[14] M. Methfessel and A. T. Paxton, Phys. Rev. B **40**, 3616 (1989).
[15] A. T. Paxton, M. Methfessel, and M. Polatoglou, Phys. Rev. B **41**, 8127 (1990).
[16] D. Ceperley and D. Adler, Phys. Rev. Lett. **45**, 566 (1980).
[17] B. Sundmann, B. Jansson, and J. O. Anderson, CALPHAD: Comput. Coupling Phase Diagrams Thermochem. **2**, 153 (1985).
[18] J. Friedel, Helv. Phys. Acta **61**, 538 (1988).
[19] C. van Reuth and R. M. Waterstrat, Acta Crystallogr., Sect. B: Struct. Crystallogr. Cryst. Chem. **24**, 186 (1968).
[20] P. E. A. Turchi and A. Finel, Phys. Rev. B **46**, 702 (1992).
[21] F. Ducastelle, in *Cohesion and Structure*, edited by F. R. de Boer and D. G. Pettifor (North-Holland, Amsterdam, 1991), Vol. 3.